J. Neurovirol. (2011) 17:559–569
DOI 10.1007/s13365-011-0064-z

A truncation mutation of the neurovirulence ICP22 protein produced by a recombinant HSV-1 generated by bacterial artificial chromosome technology targets infected cell nuclei

Robert N. Bowles · John A. Blaho

Received: 30 August 2011 / Revised: 15 November 2011 / Accepted: 17 November 2011 / Published online: 3 December 2011
© Journal of NeuroVirology, Inc. 2011

Abstract The major regulatory protein ICP22 is unique among the immediate early proteins of herpes simplex virus. Viruses deleted for ICP22 replicate well in actively dividing cells, but not in quiescent cells or certain rodent lines. Accordingly, ICP22 represents an understudied herpes simplex virus (HSV) neurovirulence marker which is absolutely essential for viral neurogrowth. We utilized the bacterial artificial chromosome methodology to create a novel ICP22 truncation mutant, termed HSV-1(BACX). The integrity of HSV-1(BACX) was confirmed by detailed polymerase chain reaction analyses and immunoblotting using anti-ICP22 antibody. HSV-1(BACX) showed a reduced replication capacity in rabbit skin cells, consistent with previous studies using ICP22-null viruses. Importantly, HSV-1(BACX) localized to nuclei of infected primate Vero cells in a manner similar to wild-type ICP22. Thus, HSV-1(BACX) will serve as a useful tool to decipher the unusual biological properties and functions of the ICP22 protein.

Keywords Herpes simplex virus · Neurovirulence · ICP22 · Bacterial artificial chromosome

Introduction

Herpes simplex viruses type 1 (HSV-1) cause a variety of infections, remain latent in its host for life, and can be reactivated to cause lesions at or near the site of infection. While the mechanism of viral reactivation from the latent state remains unclear, it is likely that the process involves the transfer of a neuronal signal to the viral replication machinery. Complete understanding of HSV infection in neurons and the reactivation from its latent state requires knowledge of the molecular mechanisms involved in the regulation of HSV replication. HSV-1 is an enveloped, double-stranded DNA virus with a genome size of approximately 152 kilobase pairs (kbp). The genome is composed of covalently linked unique long (U_L) and unique short (U_S) segments bounded on either side by inverted repeats (IR) and it encodes over 80 proteins.

Viral gene expression is coordinately regulated and sequentially ordered in a cascade fashion (Honess and Roizman 1974, 1975). The first genes transcribed are the immediate early (IE) genes which encode five infected cell proteins (ICPs), designated ICP0, ICP4, ICP22, ICP27, and ICP47. All five IE proteins perform multiple regulatory functions that affect the expression or accumulation of viral and cellular proteins during the course of viral replication (reviewed in Roizman and Knipe 2001). Synthesis of the IE proteins peaks between 3 and 5 h postinfection (hpi; Honess and Roizman 1974, 1975). The genes that are transcribed next are termed early (E) genes which encode proteins such as thymidine kinase and deoxyribonucleic acid (DNA) polymerase. The E proteins peak between 5 and 7 hpi and most function to synthesize the viral genome (reviewed in Boehmer and Lehman 1997). Finally, the late (L) genes are transcribed which encode primarily structural proteins (capsid and tegument proteins) and viral glycoproteins. The L proteins peak between 7 and 9 hpi and are required for packaging of viral DNA and assembly of the virion particles (reviewed in Enquist et al. 1998).

ICP22 is one of the five IE proteins and it has been of interest to us for the following reasons. It is the product of the U_S1 gene which is the first open reading frame (ORF) in

R. N. Bowles · J. A. Blaho (✉)
Department of Microbiology, Mount Sinai School of Medicine,
One Gustave L. Levy Place,
New York, NY 10029, USA
e-mail: john.blaho@mssm.edu

the U_S segment of the viral genome, adjacent to the internal IR (McGeoch et al. 1985). ICP22 is a protein of 420 amino acids with a predicted molecular weight of 46,522 daltons (Da) and it migrates with an apparent size of 68 kDa (Ackermann et al. 1985; Marsden et al. 1978). Although it is not essential for replication in culture (Ogle and Roizman 1999; Post and Roizman 1981), it was reported that ICP22 is required for efficient expression of E genes (Sears et al. 1985), as well as a subset of L viral genes (Purves et al. 1993), suggesting a role for ICP22 in the regulation of HSV-1 gene expression. Transient expression studies have also suggested a role for ICP22 in the regulation of IE genes (Prod'hon et al. 1996).

ICP22 is unique among the IE proteins. Viruses which contain deletions of, and insertions in, the ICP22 gene have reduced plating efficiencies in certain rodent cell lines and in primary human cell lines, but not in continuously passaged primate cell lines (Long et al. 1999; O'Toole et al. 2003; Sears et al. 1985). In addition, these viruses are highly attenuated in the central nervous system of mice (Brandt and Kolb 2003; Sears et al. 1985). Thus, ICP22 represents an understudied neurovirulent marker which is absolutely required for viral neurogrowth.

In an attempt to understand the mechanism of action of ICP22, it has been shown to modify the host ribonucleic acid (RNA) polymerase II (RNAPII; Bastian and Rice 2009; Long et al. 1999; Rice et al. 1995; Spencer et al. 1997), which is dependent on serine-2 phosphorylation (Fraser and Rice 2005, 2007). The cdk9 may be involved in this process (Durand et al. 2005; Durand and Roizman 2008). Consistent with its necessity for replication in non-dividing cells, ICP22 was reported to decrease cyclin A and B, as well increase cdc2 activity (Advani et al. 2000). Finally, visualization of ICP22 within infected cells indicates that ICP22 is needed for efficient VICE domain formation (Bastian et al. 2010).

In this study, we generated a novel ICP22 truncation mutant virus, HSV-1(BACX). We confirmed the integrity of the virus using polymerase chain reaction (PCR) and immunoblotting analyses. HSV-1(BACX) showed a reduced replication capacity in rabbit skin cells, consistent with previous studies using ICP22-null viruses. Importantly, HSV-1(BACX) localized to nuclei of infected African green monkey kidney Vero cells in a manner similar to wild-type ICP22. HSV-1(BACX) will serve as a useful tool to decipher the unusual biological properties and functions of the ICP22 protein.

Materials and methods

Cell lines and viruses

African green monkey kidney (Vero) and rabbit skin cells were obtained from the American Type Culture Collection and passaged in Dulbecco's modified Eagle medium (DMEM) supplemented with 5% fetal bovine serum (FBS). HSV-1(R325) (Post and Roizman 1981), HSV-1 (R7802), and the prototype HSV-1(F) (Ejercito, Kieff, and Roizman 1968) were provided by Bernard Roizman, University of Chicago. Recombinant R325 contains an 821 bp deletion in the ICP22 gene. HSV-1(R7802) is an ICP22 complete null virus (Ogle and Roizman 1999). HSV-1 (BAC102) is the wt HSV-1 derived from the bacterial artificial chromosome version of HSV-1(F) (Tanaka et al. 2003). To obtain virus stocks, subconfluent monolayer Vero cultures (approximately 2×10^7 cells) were inoculated with virus at a multiplicity of infection (MOI) of 0.01. All aliquots of high titer virus stocks (approximately 10^9 PFU/ml) were stored at −80° C. All virus titer determinations were performed in duplicate and MOIs used in this study were derived from the number of plaque forming units (PFU) of virus determined using Vero cells. Unless specifically indicated in the text, all biochemical reagents were obtained from Sigma.

PCR amplification of tetracycline resistance gene

The tetracycline resistance gene was PCR amplified from the Tc^R gene in the pBR322 vector plasmid (New England Biolabs). The following primers were used: forward: 5 -GGCCCTCGAGTTCTCATGTTTGACAGC3 , reverse: 5 -GGCCCTCGAGTCATCAGGTCGAGGTGGC-3 . Into both primers was incorporated an *Xho*I restriction site (underlined) and the primers anneal to the template from the consecutive bases on both primers. The forward primer anneals to nucleotides 1–17 of pBR322 to include the −35 p2 promoter sequence TTGACA; the reverse primer anneals to nucleotides 1276–1262 of the pBR322 template. Primers were obtained from IDT Technologies. The following PCR amplification cycle was used: 94°C for 5 min, followed by 40 cycles of 94°C for 1 min, 50°C for 1 min, 72°C for 1 min, with an extra ligation period for 10 min at 72°C and subsequent cooling to 4°C. The resulting 1.2 kbp product was isolated on a 1% TAE-agarose gel, excised and purified using a QIAquick PCR purification kit (QIAGEN) and then ligated to a pGEM-T vector (Promega) according to the manufacturers' protocol. Subsequent transformation into competent DH5α *Escherichia coli* (Invitrogen) and growth in tetracycline demonstrated the functionality of the cloned gene.

Insertion of Tc^R gene into ICP22

The herpes viral gene ICP22 was previously subcloned into plasmid pJB138 and contains a unique *Xho*I site (at nucleotide 877) which was used to linearize the plasmid and ligate to the complimentary sticky ends on the Tc^R gene product (O'Toole et al. 2003). The ligation product was transformed into competent DH5α *E. coli* which were grown on agar

plates containing tetracycline (50 μg/ml) to select for the insert. Resulting colonies were screened by PCR for the insert using the above amplification primers; with the PCR products analyzed on a 1% agarose gel. Clones (seven) containing insert were then amplified in 3 ml cultures of Luria broth (LB; containing tetracycline) overnight at 37°C with shaking. Bacterial cells were pelleted and DNA-purified (Qiagen miniprep) and digested with *Xho*I and checked for the presence of insert on a 1% agarose gel. Five miniprep cultures showed the presence of insert and were made 10–15% in glycerol and stored at −80°C.

Determination of correct orientation of insert of Tc^R gene into ICP22

It was important to us that the insert was not colinear with the ICP22 so that no potential fusion between the two proteins might occur. As the insert is flanked with *Xho*I sticky ends, the orientation of ligation maybe either in the desired position, or it may assume the reverse orientation. To ascertain which orientation in the clone the insert has assumed, DNA from the five minipreps above were digested with both *Xho*I and *Hin*dIII. The difference between the orientations of insert is seen with the *Hin*dIII digest. This produces an 8.2 kb fragment where the insert is in the "reverse" position, whereas with clones of the desired orientation, this digestion produces a band of approximately 7 kb.

Preparation of JC8679 cells and transformation with BAC102

Freeze-dried JC8679 cells (recE, recT) (Life Technologies) were reconstituted in SOB medium and plaque-purified on an agar plate containing 20 μg/ml of streptomycin. Picked colonies were amplified overnight in 3 ml of LB containing streptomycin at 37°C with shaking. One miniprep culture was then further amplified by inoculation of 0.8 ml into 200 ml of LB in a 1 l shaker flask containing streptomycin and incubating at 30°C with shaking until an OD600 of 0.4–0.5 was reached (approximately 5 ½h). Cells were transferred to 50 ml Falcon tubes and incubated on ice for several hours. This was followed by washings in cold glycerol solution to render the cells electrocompetent.

An *E. coli* culture containing a bacterial artificial chromosome incorporating the full-length HSV-1 genome (pYEBAC102; Tanaka et al. 2003) was colony-purified on an agar plate containing chloramphenicol (170 μg/ml) and then amplified in LB. Bacterial cells from the maxiprep culture were pelleted and plasmid (BAC102) DNA extracted using a Qiagen maxiprep kit. To 50 μl of the above electrocompetent JC8679 cells was added 8 μl of BAC102 DNA (approximately 50 ng/μl) and mixed. The suspension was transferred to a 0.1 cm cuvette and electroporated (1.8 kV with time constant for 412 ms) then added to 300 μl of SOB medium and left on ice for 2 min. After incubation for 3 h at 37°C with shaking, the transformed cells were plaque-purified on agar containing 170 μg/ml chloramphenicol to select for the presence of BAC102. To confirm the successful transformation of JC8679 cells, BAC102 DNA was isolated from a miniprep culture using a NucleoBond BAC Maxi Kit (Clontech) and digested with *Bam*HI. When run on an agarose gel, a characteristic ladder was produced (result not shown). Glycerol stocks were made of the transformed cells.

One step replacement of ICP22 in HSV-BAC with ICP22 insertion mutation

One clone of pJB138 containing the Tc^R gene inserted into ICP22 in the desired orientation was selected for amplification. Purified DNA was digested with *Nco*I to produce a linearized 5.2 kb fragment containing the mutated ICP22 gene, and this fragment was isolated on a 1% agarose gel and purified using a Qiagen minicolumn.

To 50 μl of BAC102-transformed JC8679 cells which had been made electrocompetent was added purified *Nco*I digest. Electroporation was performed as above before plating on agar containing chloramphenicol and tetracycline to select for homologously recombined HSV-BAC clones containing the Tc^R gene inserted into ICP22. All 17 colonies which grew were amplified overnight in 3 ml of LB containing chloramphenicol and tetracycline and then screened by PCR for the presence of the Tc^R gene insert. The 15 minipreps demonstrating presence of the BAC carrying the introduced mutation (BACX) were amplified in 250 ml of LB containing chloramphenicol, streptomycin, and tetracycline and rescreened by PCR for the presence of insert.

Production of mutant virus

DNA from maxipreps where PCR screening demonstrated the presence of the ICP22 mutation was used to transfect subconfluent Vero cells in 25 cm^2 flasks using a calcium chloride transfection protocol described previously (O'Toole et al. 2003). Cells were incubated at 37°C until plaques appeared whereupon the medium was aspirated and the cells overlayed with 1% agarose in PBS. Picked plaques were transferred to a milk solution and sonicated to release virus particles (Blaho et al. 2005). These were amplified by infecting subconfluent Vero cells in 25 cm^2 flasks until 100% CPE was achieved to give a low titer virus stock. A second round of amplification using cells in a 75 cm^2 flask produced a high titer stock virus.

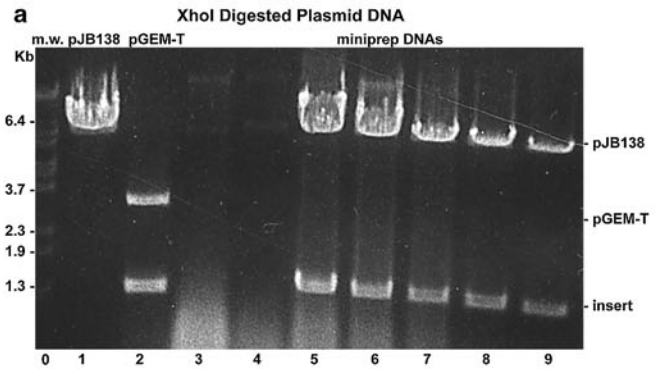
a
XhoI Digested Plasmid DNA
m.w. pJB138 pGEM-T
miniprep DNAs
Kb
6.4
3.7
2.3
1.9
1.3
pJB138
pGEM-T
insert
0 1 2 3 4 5 6 7 8 9

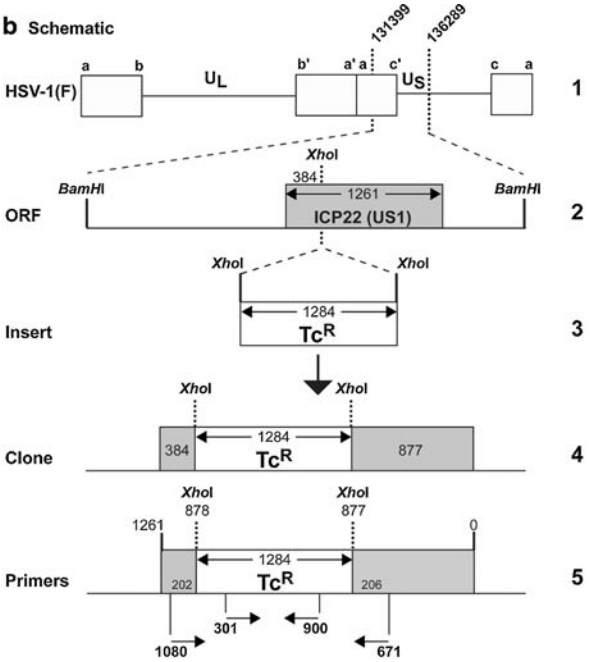
b Schematic
131399
136289
HSV-1(F)
a b
UL
b' a' a c'
US
c a
1
XhoI
384
1261
BamHI
BamHI
ORF
ICP22 (US1)
2
XhoI
XhoI
1284
TcR
Insert
3
XhoI
XhoI
384
1284
TcR
877
Clone
4
XhoI
878
XhoI
877
1261
0
1284
202
TcR
206
Primers
5
301
900
1080
671

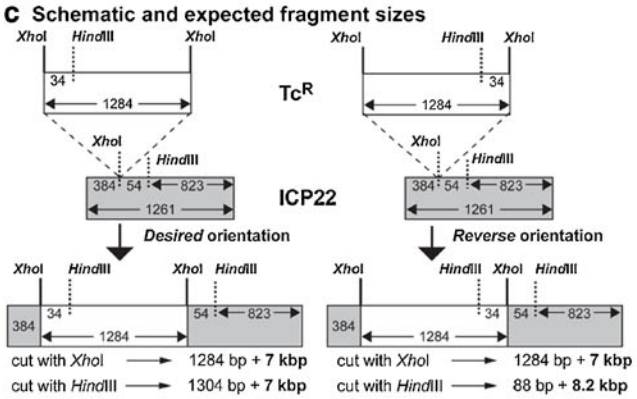
c Schematic and expected fragment sizes
XhoI HindIII XhoI
34
1284
TcR
XhoI
HindIII
384 54 823
1261
ICP22
Desired orientation
Reverse orientation
384
54
823
cut with XhoI → 1284 bp + 7 kbp
cut with HindIII → 1304 bp + 7 kbp
cut with XhoI → 1284 bp + 7 kbp
cut with HindIII → 88 bp + 8.2 kbp

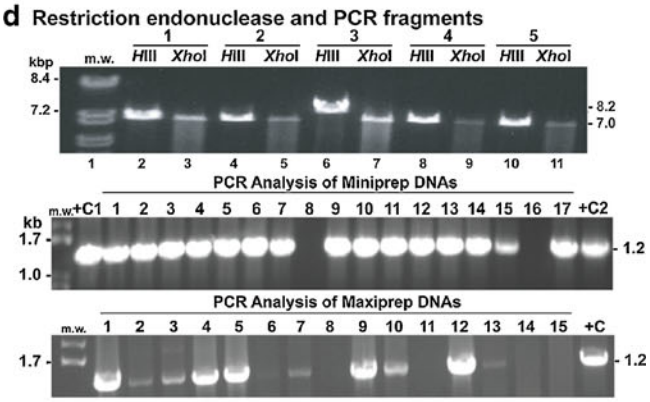
d Restriction endonuclease and PCR fragments
1 2 3 4 5
HIII XhoI
kbp
m.w.
8.4
7.2
8.2
7.0
1 2 3 4 5 6 7 8 9 10 11
PCR Analysis of Miniprep DNAs
m.w. +C1 1 2 3 4 5 6 7 8 9 10 11 12 13 14 15 16 17 +C2
kb
1.7
1.0
1.2
PCR Analysis of Maxiprep DNAs
m.w. 1 2 3 4 5 6 7 8 9 10 11 12 13 14 15 +C
1.7
1.2

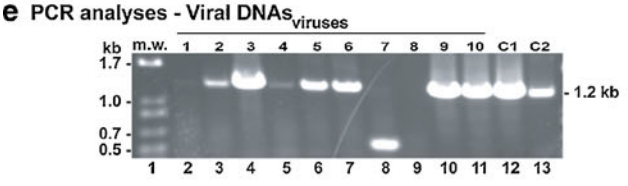
e PCR analyses - Viral DNAs
viruses
kb
m.w.
1 2 3 4 5 6 7 8 9 10 C1 C2
1.7
1.0
0.7
0.5
1.2 kb
1 2 3 4 5 6 7 8 9 10 11 12 13

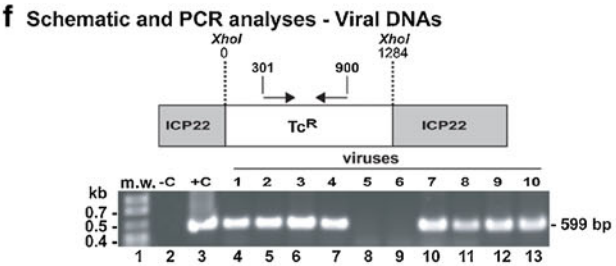
f Schematic and PCR analyses - Viral DNAs
XhoI
0
301
900
XhoI
1284
ICP22
TcR
ICP22
viruses
kb
m.w. -C +C 1 2 3 4 5 6 7 8 9 10
0.7
0.5
0.4
599 bp
1 2 3 4 5 6 7 8 9 10 11 12 13

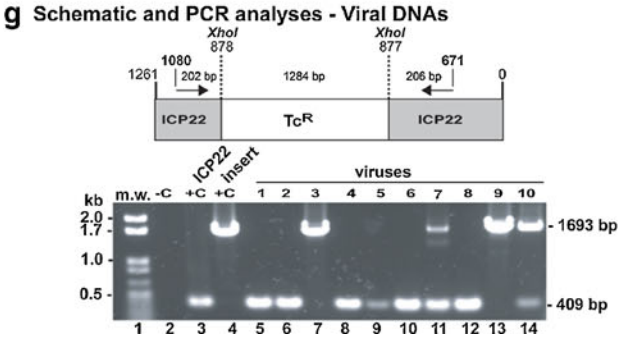
g Schematic and PCR analyses - Viral DNAs
XhoI
878
XhoI
877
1080
671
1261
202 bp
1284 bp
206 bp
0
ICP22
TcR
ICP22
ICP22 insert
viruses
kb
m.w. -C +C +C 1 2 3 4 5 6 7 8 9 10
2.0
1.7
1.0
0.5
1693 bp
409 bp
1 2 3 4 5 6 7 8 9 10 11 12 13 14

Fig. 1 **a** Fluorescence enhancement image of recombinant plasmids containing Tc^R gene. Electrophoretically separated DNA fragments were stained with ethidium bromide and visualized as described in "Materials and methods." *Lane 1*: pJB138 vector containing the ICP22 gene linearized with *Xho*I restriction endonuclease. *Lane 2*: pGEM-T vector containing Tc^R gene insert digested with *Xho*I. *Lanes 3–9*: Candidate DNA samples digested with *Xho*I. "Insert" refers to the *Xho*I fragment containing the tetracycline resistance gene (Tc^R). **b** Schematic representation of the HSV genome and ICP22 constructs utilized in this study. The wild-type HSV-1 genome in the prototype orientation is shown in *line 1*. The unique long (U_L), unique short (U_S), and terminal repeat segments (*a*, *b*, *c*, *a*', *b*', *c*') are indicated. The coordinates of the *Bam*N fragment in the viral genome are indicated and these regions are expanded in *line 2*. *Line 2*: The predicted ORF of ICP22 in the BamN regions of wild-type virus. The length of the ICP22 (bp) is 1261 and a unique *Xho*I site is located 384 bp in from the start of ICP22. *Lane 4*: Insertion mutation construct (Clone) containing the Tc^R gene fragment (1284 bp) inserted into the unique *Xho*I site in ICP22. *Line 5*: *Arrows* mark the locations and orientations of primers used for PCR screening and mutagenesis analyses. Coordinates run from 0 to 1261 bp of the ICP22 ORF. "301" and "900" represent arbitrary nucleotide positions within the TcR insert that mark the locations of PCR primers amplify, thus giving a 599 bp segment. "202" and "206" refer the number of ICP22 bps included in the product from the outer pair of primers ("1080" and "671") thus yielding a 1693 bp product (1284 bp +202 bp+206 bp+1 bp) if the Tc^R insert is present or a 409 bp product (202 bp+206 bp+1 bp) if it is absent. Schematic representation showing polarities and expected fragment sizes of Tc^R insertion in ICP22. As the cleaved Tc^R insert is flanked by *Xho*I sticky ends it may ligate in either the desired orientation where its direction of transcription is the same as that of ICP22, or it may ligate in the opposite orientation. The desired orientation of the insert is to prevent the possibility of a fusion protein (truncation and insert) being formed. **c** The schematic demonstrates that digestion by *Hin*dIII can differentiate between these two polarities; with the Tc^R insert in the desired orientation a 7 kbp fragment is produced and when in the reverse orientation an 8.2 kbp fragment is produced. **d** Fluorescence enhancement image of PCR products derived from recombinant plasmids. *Top panel*: Five representative miniprep DNA preparations (1–5) were digested separately with *Hin*dIII and *Xho*I, electrophoretically separated on an agarose gel, and visualized by fluorescence enhancement following staining with ethidium bromide. *Middle panel*: DNA samples derived from small liquid (miniprep) cultures. Bacterial colonies that grew on chloramphenicol and tetracycline containing agar after plating cells from the homologous recombination procedure between Bac102 and the insertionally mutated ICP22 gene were screened by PCR for the presence of the Tc^R insert. Electrophoretically separated PCR DNA fragments were stained with ethidium bromide and visualized as described in "Materials and methods." "C+1" refers to pGEM-T vector containing Tc^R insert. "C+2" refers to the ICP22 vector pJB138 containing the Tc^R insert. *Panel d, bott*om. Each of the 15 miniprep DNA samples demonstrating presence of the homologous recombination product (1.2 kb PCR fragment) were amplified in 250 ml of media (Maxiprep) containing chloramphenicol, streptomycin and tetracycline and rescreened by PCR for the presence of the Tc^R gene insert. "C+" is pGEM-T vector containing the Tc^R insert. Fluorescence enhancement images of PCR products derived from recombinant viral DNAs (**e**–**g**). Viral DNA was extracted from viruses 1 to 10 (Fig. 4) was analyzed by PCR as described in "Materials and methods." **e** Viral DNAs were tested for the presence of the insert (1.2 kb) using the Tc^R amplification primers. *C1* refers to the pGEM-T vector containing the Tc^R insert, *C2* refers to the ICP22 vector pJB138 containing the Tc^R insert. **e** Unique primers (schematic) were used to amplify a 599 bp internal portion of the TcR insert from the viral DNAs. *-C* refers to the negative control containing no DNA template, *+C* refers to the positive control pGEM-T vector containing the Tc^R insert. **g** Unique flanking primers which amplify forward and backward within ICP22 (schematic) were utilized amplify the TcR insert from the viral DNAs; a 1,693 bp fragment product indicates that the TcR insert is present within ICP22, and a 409 bp fragment indicates that it is not

Screening virus for ICP22 insertional mutation

Subconfluent Vero cells were infected with mutant virus until 100% CPE was achieved. Cells were scraped and pelleted (nuclear fraction) and the supernatant transferred to another tube (cytoplasmic fraction). Lysates from pellets were separated on a 10% SDS gel and the presence of ICP22 determined by Western blot analysis as previously described (Blaho et al. 2005; O'Toole et al. 2003). The blot was also probed for ICP8 and actin as infection and loading controls respectively. A second blot using the same lysates and probed for only ICP8 and ICP22 to allow visualization of truncated ICP22 protein was also performed. Details are provided below.

The cytoplasmic fraction containing nascent virus was enriched for viral DNA using a chloroform/phenol extraction procedure and the purified DNA subsequently subjected to three PCR assays to determine the presence or otherwise of the tetracycline resistance gene. Firstly, PCR was performed with the tetracycline resistance gene amplification primers, with a 1.2 kb product indicative of the virus containing the manufactured mutation. A second round of PCR involved targeting the internal portion of the Tc^R gene using the following primers: forward: 5′-CCGCCCAGTCCTGCTCGCTT-3′, reverse: 5′-TTGGTGGCGGGACCAGTGAC-3′ which amplifies a 599 bp fragment from base 301 to 900. The third PCR assay amplifies forward from base 671 of ICP22 and back from base 1080 of ICP22 using the following primers: forward 5′-ACTGTTACCTGATGGGATAC-3′, and reverse 5′-CTGGG GGGTCCAGTCAAACT-3′. The presence of the insert in ICP22 will yield a product of 1693 bp, and where the insert is not present, the product will be a small amplified portion of ICP22 of 409 bp.

Western blotting

Protein samples (50 μg) was separated on a 12% SDS gel with a 6% stacking gel (Blaho and Roizman 1998) along with prestained molecular mass markers (Gibco) and transferred to a Protran nitrocellulose membrane (Schleicher and Schuell) in a tank apparatus (Bio-Rad) for 1 h at 100 V and 4°C. The blots were then blocked in 5% nonfat dried milk (Carnation) in PBS for 1 h. After blocking, membranes were washed in PBS to remove excess milk before incubating in primary antibody for 1 h. After rinsing three times in Tris-buffered saline (TBS), 0.1% Tween (100 mM NaCl, 10 mM Tris–HCl, pH 7.5, and 0.1% Tween 20), the blots were then incubated in a secondary antibody for 1 h. A further rinsing in TBS and 0.1% Tween was followed by rinsing in TBS

and then washing once for 5 min in 100 mM Tris–HCl, pH 9.5, 100 mM NaCl, and 5 mM $MgCl_2$. The blot was then incubated in a developer (p-nitroblue tetrazolium and 5-bromo-4- chloro-3-indolyl phosphate; Gibco) until the protein bands could be visualized. The blots were scanned using an AGFA Arcus II scanner and organized using Adobe Photoshop and Adobe Illustrator. The blots remain graphically unmodified. Primary antibodies were: anti-ICP8 antibody (gift of Bill Ruyechan), rabbit polyclonal anti-ICP22 antibody (RGST22; Blaho et al. 1997), and anti-actin antibody (Sigma). Secondary goat anti-rabbit and goat anti-mouse antibodies conjugated with alkaline phosphatase were purchased from Southern Biotechnology. Primary antibodies were used at a dilution of 1:1000 in PBS containing 1% BSA and secondary antibodies were used at a dilution of 1:1000 in PBS containing 5% milk.

Indirect immunofluorescence

Infected Vero cells were prepared for indirect immunofluorescence as described previously (Pomeranz and Blaho). Primary antibodies: mouse anti-tubulin (1:500), rabbit anti-ICP22 (1:500), mouse anti-ICP4 (1:500) in 1%BSA/PBS Secondary antibodies: anti-rabbit-FITC (1:300), anti-mouse-TxRd (1:100) in 1%BSA/PBS.

Virus replication study

Burst size experiments were performed as described previously (O'Toole et al. 2003; Pomeranz and Blaho 2000). Vero and rabbit skin cells were infected at a MOI of 5.0. Virus stocks were prepared 24 hpi and titered in duplicate using Vero cells.

Results

Generation of truncated ICP22 fragment

We set out to create a novel ICP22 truncation mutant recombinant virus using bacterial artificial chromosome technology. As detailed in the "Materials and methods," the tetracycline resistance gene (Tc^R) was successfully amplified by PCR from the pBR322 plasmid using primers designed to incorporate two *Xho*I sticky ends into the product. This product was then ligated to a pGEM-T vector and subsequently used to transform competent DH5α *E. coli* cells, which, when amplified in culture containing tetracycline, demonstrated the functionality of this cloned gene (data not shown). Using the complimentary sticky *Xho*I ends, the gene was then subcloned into the unique *Xho*I restriction site within the ICP22 ORF contained in the pJB138 plasmid (Fig. 1b). Again, competent DH5α *E. coli* cells were transformed with this plasmid and selected on tetracycline plates. Colonies which subsequently grew were screened for the insert by PCR using the original amplification primers and seven colonies demonstrating its presence were amplified in miniprep culture. Plasmid was then purified from the pelleted cells, digested with *Xho*I and analyzed on an agarose gel for the presence of insert. Five minipreps contained the clone (Fig. 1a, lanes 5–9). These clones were then further analyzed for their orientation of the inserts (Fig. 1b and c) by performing a *Hin*dIII digest, which showed one of the clones, clone 3, contained the insert in the "reverse" orientation (Fig. 1d, top). Clone 1 (Fig. 1d) was selected for amplification. As described in "Materials and methods," this purified plasmid DNA was finally digested with *Nco*I to produce a linearized 5.2 kbp fragment containing the mutated ICP22 gene, which was subsequently isolated and purified to be used in the generation of the recombinant virus.

Fig. 2 Immunoblot images of ICPs (**a**, **c**). Ten independent viruses were produced following unique transfections of Vero cells with recombinant bacterial artificial chromosome DNA containing the Tc^R gene inserted into ICP22. **a** Lysates from Vero cells infected by each of the ten viruses were electrophoretically separated on a 12% denaturing gel, electrically transferred to nitrocellulose, and probed with antibodies against ICP22, ICP8, and cellular actin as described in "Materials and methods;" the latter two were used as controls for infection and sample loading, respectively. **b** Schematic of Tc^R gene inserted into ICP22 showing orientation of ICP22. These are positions on the ICP22 gene counting from left to right as depicted in Fig. 2b. *Xho*I is at position 877, and *Hin*dIII at 823 if counting from right to left. **c** The ten lysates in panel **A** were loaded onto a duplicate gel as shown in panel **A** except that additional control extracts were loaded and the polypeptides were electrophoretically separated for half the amount of time to allow detection further down the blot of truncated ICP22. *Lane 1*: Lysate from mock-infected cells. *Lane 2*: Lysate from HSV-1(F)-infected cells. *Lane 3*: Lysate from parental Bac102-derived virus-infected cells. *Lane 4*: Lysate from ICP22-null R7802 virus-infected cells. *Lane 5*: Lysate from ICP22-truncated R325 virus-infected cells. *Lanes 6–15*: Lysates from cells infected by recombinant viruses 1–10 (−). *m.w.* refers to locations of molecular weight markers (kDa). Locations of the R325-derived, truncated ICP22, and the novel ICP22 truncations (BACX) are indicated in the *left* margin. **d** Virus burst size calculations for HSV-1(F), HSV-1(BACX), and HSV-1(BAC102) infect Vero and rabbit skin cells. Duplicate cultures of Vero and rabbit skin cells were infected with identical amounts (MOI=0.5 and 5.0) of HSV-1(F), HSV-1(BACX), and HSV-1(BAC102) virus. At 24 hpi, virus stocks were prepared and the amounts of infectious virus in each preparation was determined by virus titering on Vero cells, as described in "Materials and methods." Values are the average of two parallel experiments (N=2). The results shown are for the MOI=5.0 experiment

Generation of recombinant HSV-1 producing a truncated ICP22

Plaque-purified JC8679 cells which, after being rendered electrocompetent by washing in cold glycerol solution, were electroporated with BAC102 DNA, a bacterial artificial chromosome containing the full-length HSV-1 genome.

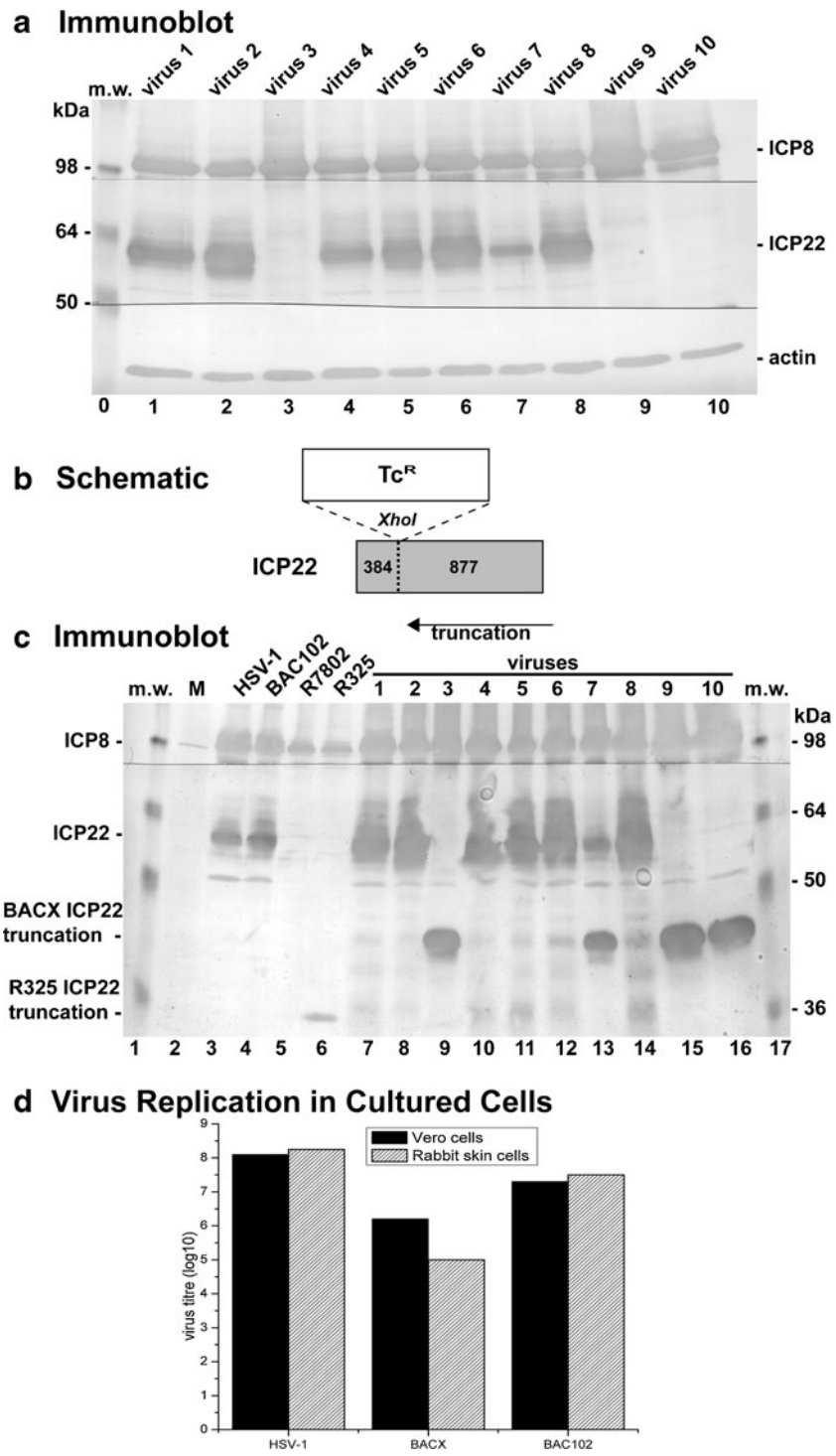

Transformed JC8679 cells, after amplification, were again made electrocompetent, to facilitate the uptake of the *Nco*I fragment containing the mutated ICP22 gene (described in section above). Homologously recombined HSV-BAC clones containing the Tc^R gene inserted into ICP22 ORF were selected for by plating on agar containing chloramphenicol and tetracycline. All 17 colonies which grew were amplified overnight in 3 ml of LB containing chloramphenicol and tetracycline and then screened by PCR for the presence of the Tc^R insert (Fig. 1d, middle). The 15 minipreps which demonstrated the presence of the introduced mutation (BACX) were maxiprepped in 250 ml cultures and rescreened by PCR for the presence of the insert to reveal eleven recombinant clones (Fig. 1d, bottom).

Transfection of subconfluent Vero cells with DNA from these eleven clones gave rise to ten viral plaques which were purified and further amplified in Vero cells to give ten high-titer recombinant HSV-1 stocks.

Confirmation of recombinant virus by PCR

Recombinant viruses were used to infect Vero cells and viral DNA was isolated and subjected to PCR analyses. Three separate characterizations were performed. The Tc^R gene amplification primers were used to screen for this insert (Fig. 1g, top). Of the ten recombinant viruses, viruses 3, 9, and 10 showed the greatest amount of the Tc^R gene (Fig. 1e, lanes 4, 10, and 11). Virus 7 produced what looks like a fragmented gene while virus 8 showed no insert whatsoever (Fig. 1e, lane 8). The next PCR screen targeted a 599 bp internal portion of the Tc^R gene (Fig. 1f, top). Viruses 5 and 6 produced no fragment in this screen (Fig. 1f, lanes 8 and 9). The third PCR screen employed primers targeting the internal portions of the fragmented ICP22 gene either side of the insertion, thus indicating whether the Tc^R gene was still present as the original clone within the ICP22 ORF (Fig. 1g, top). Only viruses 3, 7, 9, and 10 produced the larger fragment of 1693 bp, indicating they have the correct insertional mutation, but the fragment for virus 7 is much reduced in intensity as compared to the other three viruses (Fig. 1g, compare lanes 7, 13, and 14 with 11). The smaller fragment of 409 bp, indicating no insertion of Tc^R gene into ICP22 was seen in all viruses except 3 and 9, but including virus 7 (Fig. 1g).

Immunoscreening of recombinant virus

The cytoplasmic fractions of the cell lysates used above (Fig. 1e, f and g) were utilized for immunoblotting analyses. As described in "Materials and methods," the recombinant viruses were tested for the presence or absence of ICP22. Of the ten generated recombinant viruses, three showed a complete absence of the full-length ICP22 protein (Fig. 2a, lanes 3, 9, and 10). Further immunoblot analyses reveals these three ICP22-null viruses produced a truncated ICP22 protein of approximately 45 kDa (Fig. 2c, lanes 9, 13, 15, and 16), corresponding to an ICP22 truncation mutant of 384 nucleotides (Fig. 2b). The results indicated that the 384-nucleotide deletion yeilded an ICP22 truncation that migrates at approximately 45 kDa. This is comparable to the R325 ICP22 mutant virus that has a 500 bp deletion in Us1 but produces a protein of approximately 35 kDa. Based on this immunoblot data and the previous PCR characterizations (Fig. 1e, f and g), virus 3 was selected as the prototype recombinant virus for the rest of this study. This virus was designated as HSV-1(BACX).

Fig. 3 Indirect immunoflourescence staining of infected Vero cells. ▶ Vero cells were Mock-, HSV-1(F)-, HSV-1(BAC102)-, HSV-1 (R7802)-, and HSV-1(BACX)-infected and processed for indirect immunofluorescence using anti-ICP4, -ICP22, and control-tubulin antibodies as described in "Materials and methods." Infected cells were also stained with Hoechst dye to identify nuclei. *Top panel*: Hoechst, ICP4, ICP22 images with overlays of ICP4/ICP22 and Hoescht/ICP4/ICP22. *Bottom panel*: Immunostaining for tubulin and ICP22, showing the overlay

Surprisingly, recombinant virus 7 showed detectable full-length ICP22 expression, as well as the presence of truncated protein (s. 2 C, lane 13). We also observed a unique fragment with this virus when screening with the Tc^R gene amplification primers Fig. 1g, lane 11), but not one corresponding to the 1.2 kbp insert (Fig. 1e, lane 8). It is also interesting to note that other recombinant viruses (viruses 1, 2, 4, and 8) showed the presence of the insert (Fig. 1f) but have full-length ICP22 protein (Fig. 2a), suggesting the Tc^R gene has inserted itself into another part of the viral genome. Such a secondary insertion elsewhere in the viral genome might explain how virus 7 is able to produce both full-length and truncated ICP22. While it is always possible that this could occur through a mixed stock of potentially wild-type and mutant viruses, we feel this is an unlikely. Consider the fact that the full-length and truncated proteins are produced in considerably smaller quantites than the other viruses, along with the anomalies in the PCR analyses of virus 7 (Fig. 1e and g). Anomalies with other viruses are also evident where the PCR analyses show the presence of inserts but the immunoblot analyses reveal only full-length protein (viruses 1, 2, 4, and 8). These observations imply that some unknown process may have taken place during the homologous recombination event which we do not understand and teaches caution when using BAC technology.

Replication defect of ICP22 truncation recombinant virus BACX

To determine the consequence of the truncation of the ICP22 protein expressed by the BACX virus, we directly compared BACX growth in restrictive rabbit skin cells with that in permissive Vero cells. Subconfluent Vero and rabbit skin cell cultures were infected in duplicate with wt HSV-1, wt Bac102-derived HSV-1, and recombinant BACX at MOIs of 0.5 (data not shown) and 5. At 24 h postinfection, virus stocks were generated from the infected cells and the degree of virus growth in each culture was determined by subsequent titering on Vero cells. The results (MOI=5.0) with the control wt HSV-1 s for both MOIs reflected a similar pattern showing that the Bac102-derived virus grew to within approximately half a log of the standard HSV-1 virus in both cell types (Fig. 2d, compare HSV-1 with BAC 102). Importantly, the BACX mutant virus demonstrated

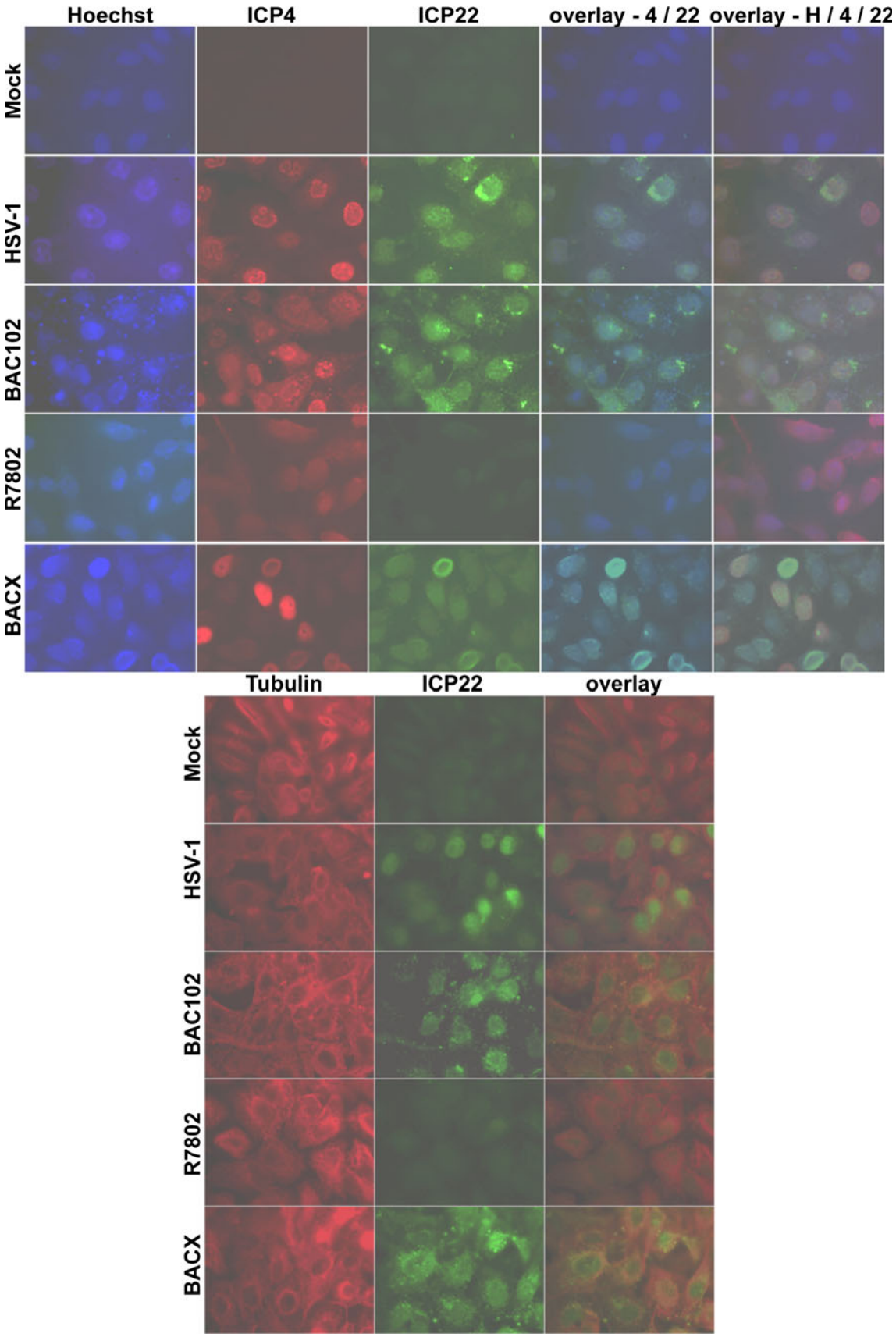
Hoechst
ICP4
ICP22
overlay - 4 / 22
overlay - H / 4 / 22
Mock
HSV-1
BAC102
R7802
BACX
Tubulin
ICP22
overlay
Mock
HSV-1
BAC102
R7802
BACX

retarded growth in both cell types. In Vero cells, this growth defect represented an approximate 2 log decrease in PFU while in rabbit skin cells it was more marked, at approximately a 3 log difference. Based on these results. We conclude that the recombinant BACX virus displays a growth defect in rabbit skin cells as a result of the truncation of the ICP22 gene.

Indirect immunofluorescence of truncated ICP22 during productive BACX virus infection

The previous results demonstrated a biological effect of the ICP22 truncation in the BACX recombinant virus. The final goal of this study was to determine the subcellular localization of the truncated ICP22 during productive infection. Permissive Vero cells were mock infected or infected BACX. Controls included wt HSV-1 and wt BAC102, as well as the ICP22 complete null virus, R7802. At 24 hpi, the infected cells were prepared for indirect immunofluorescence studies using antibodies targeting ICP22, ICP4 and cellular tubulin, as described in "Materials and methods."

As expected, full-length ICP22 produced during the wt HSV-1 infections accumulated in infected cell nuclei (Fig. 3). No immune reactivity was observed with R7802. ICP4 staining (Fig. 3, top) demonstrated the infectivity of BACX. Interestingly, truncated ICP22 produced by BACX was detected in nuclei and produced a similar localization pattern as full-length ICP22 produced by the wt HSV-1 s. This is further demonstrated in the overlay panels of with ICP22 and Hoechst staining. Truncated ICP22 from BACX also colocalized with ICP4 as observed in the ICP22 and ICP4 overlays. Finally, truncated ICP22 did not colocalize with cytoplasmic tubulin (Fig. 3, bottom). Based on these results, we conclude that the truncated ICP22 produced by the recombinant BACX virus translocates to nuclei in a manner similar to that of full-length ICP22 during productive virus infection.

Discussion

The ICP22 protein of HSV-1 is of interest because it represents an understudied neurovirulent marker which is absolutely required for viral neurogrowth. The purpose of this study was to generate a novel truncated ICP22 protein that is expressed within the context of the viral genome using the bacterial artificial chromosome technology. The key findings of our study may be summarized as follows.

The virus, termed BACX, which synthesizes an approximately 45 kDa truncated form of ICP22 has a replication defect in rabbit skin cells compared to that in Vero cells. The growth defect is less that that observed with a complete ICP22-null virus. We cannot exclude the possiblity that the growth defect is due to an undetectable lesion outside of the ICP22 locus. Repair of the truncation virus back to wild type will address this. The inability of ICP22 mutant viruses to be restricted for growth in nonprimate, rodent cells has directly correlated with the reduced neurovirulence of these viruses (Brandt et al. 2003; Ogle and Roizman 1999; Poffenberger et al. 1994; Sears et al. 1985). Thus, we predict that the BACX recombinant virus would demonstrate reduced neurovirulence when it is utilized in relevant animal systems.

The truncated form ICP22 translocates to the nuclei of infected cells during productive BACX infection. This finding suggests that even though the truncated ICP22 was able to enter the nucleus, some other defect in the protein is responsible for the reduced growth of BACX in the rabbit skin cells. Importantly, our results are consistent with those of Bastian and Rice (2009) who showed that N-terminal half of ICP22 is needed for its localization to nuclear body structures. In addition, these authors identified a region in the C-terminal half of ICP22 (residues 240 to 340) that is critical for Pol II modification. We have results (Bowles and Blaho, unpublished) showing co–localization of ICP22 with RNAPII along with other viral proteins in replication compartments, as well as showing that wt virus but not R325 converts RNAPIIo to RNAPIIi. Additional studies are required to assess whether the truncated ICP22 remains functional for modifying RNAPII. It is conceivable that the ICP22 truncation defect is due to its potential lack of functional association with cyclins and cdks. However, we cannot exclude the possibility that another, yet undetermined, function of ICP22 has been affected by the truncation present in the BACX virus. For this reason, BACX may likely serve as useful tool for characterizing ICP22 function in the future.

This recombinant ICP22 mutation is unique from others that have been reported since it generates a truncated ICP22 which migrates to nuclei. BACs are very stable, enabling the virus to be easily stored and produced. As the viral genome is accessible to the tools of bacterial genetics, the generation of further desired mutations of this virus can be made much more readily in this system than in mammalian cells. ICP22 knockouts do not replicate in quiescent cells, suggesting that ICP22 is essential to the virus for neural growth. For this reason, this virus therefore may contribute to additional HSV neurovirulence studies.

Finally, based on the data presented in this study, we conclude that the carboxy terminal 128 amino acids of ICP22 are important determinants for HSV-1 cell tropism. It is conceivable that a unique functional domain resides in this portion of ICP22. The development of appropriate biochemical and molecular systems will be needed to address this and other important issues related to ICP22 function in neurovirulence.

Acknowledgments We thank (i) Jamie Yedowitz and Washington Cardenas (Mount Sinai School of Medicine) for expert technical assistance; (ii) Yasushi Kawogawa (Tokyo University) for the pYEBAC102 bacterial artificial chromosome construct; (iii) Bernard Roizman (University of Chicago) for providing low passage isolates of HSV-1(R7802) that was originally generated by William Ogle in his laboratory (Ogle and Roizman 1999), HSV-1(R325) that was originally generated by Leonard Post in his laboratory (Post and Roizman 1981), and its parental HSV-1(F). These studies were supported in part by grants from the United States Public Health Service (AI38873 and AI48582) and the American Cancer Society (JFRA 634). J.A.B. thanks the Lucille P. Markey Charitable Trust and the National Foundation for Infectious Diseases for their support.

References

Ackermann M, Sarmiento M, Roizman B (1985) Application of antibody to synthetic peptides for characterization of the intact and truncated alpha 22 protein specified by herpes simplex virus 1 and the R325 alpha 22- deletion mutant. J Virol 56:207–215

Advani SJ, Brandimarti R, Weichselbaum RR, Roizman B (2000) The disappearance of cyclins A and B and the increase in activity of the G(2)/M-phase cellular kinase cdc2 in herpes simplex virus 1-infected cells require expression of the alpha22/U(S)1.5 and U(L)13 viral genes. J Virol 74:8–15

Bastian TW, Rice SA (2009) Identification of sequences in herpes simplex virus type 1 ICP22 that influence RNA polymerase II modification and viral late gene expression. J Virol 83:128–139

Bastian TW, Livingston CM, Weller SK, Rice SA (2010) Herpes simplex virus type 1 immediate-early protein ICP22 is required for VICE domain formation during productive viral infection. J Virol 84:2384–2394

Blaho JA, Zong CS, Mortimer KA (1997) Tyrosine phosphorylation of the herpes simplex virus type 1 regulatory protein ICP22 and a cellular protein which shares antigenic determinants with ICP22. J Virol 71:9828–9832

Blaho JA, Roizman B (1998) Analyses of HSV proteins for posttranslational modifications and enzyme functions. In: Brown SM, Maclean AR (ed) Methods in Molecular Medicine: Herpes Simplex Virus Protocols, vol. 10. Human Press Inc., Totowa, pp 237–256

Blaho JA, Morton ER, Yedowitz JC (2005) Herpes simplex virus: propagation, quantification, and storage. Curr Protoc Microbiol, Chap 14:Unit 14E 1

Boehmer PE, Lehman IR (1997) Herpes simplex virus DNA replication. Annu Rev Biochem 66:347–384

Brandt CR, Kolb AW (2003) Tyrosine 116 of the herpes simplex virus type 1 IEalpha22 protein is an ocular virulence determinant and potential phosphorylation site. Invest Ophthalmol Vis Sci 44:4601–4607

Brandt CR, Kolb AW, Shah DD, Pumfery AM, Kintner RL, Jaehnig E, Van Gompel JJ (2003) Multiple determinants contribute to the virulence of HSV ocular and CNS infection and identification of serine 34 of the US1 gene as an ocular disease determinant. Invest Ophthalmol Vis Sci 44:2657–2668

Durand LO, Roizman B (2008) Role of cdk9 in the optimization of expression of the genes regulated by ICP22 of herpes simplex virus 1. J Virol 82:10591–10599

Durand LO, Advani SJ, Poon AP, Roizman B (2005) The carboxyl–terminal domain of RNA polymerase II is phosphorylated by a complex containing cdk9 and infected–cell protein 22 of herpes simplex virus 1. J Virol 79:6757–6762

Ejercito PM, Kieff ED, Roizman B (1968) Characterization of herpes simplex virus strains differing in their effects on social behaviour of infected cells. J Gen Virol 2:357–64

Enquist LW, Husak PJ, Banfield BW, Smith GA (1998) Infection and spread of alphaherpesviruses in the nervous system. Adv Virus Res 51:237–347

Fraser KA, Rice SA (2005) Herpes simplex virus type 1 infection leads to loss of serine-2 phosphorylation on the carboxyl-terminal domain of RNA polymerase II. J Virol 79:11323–11334

Fraser KA, Rice SA (2007) Herpes simplex virus immediate-early protein ICP22 triggers loss of serine 2-phosphorylated RNA polymerase II. J Virol 81:5091–5101

Honess RW, Roizman B (1974) Regulation of herpesvirus macromolecular synthesis: I. Cascade regulation of the synthesis of three groups of viral proteins. J Virol 14:8–19

Honess RW, Roizman B (1975) Regulation of herpesvirus macromolecular synthesis: sequential transition of polypeptide synthesis requires functional viral polypeptides. Proc Natl Acad Sci USA 72:1276–1280

Long MC, Leong V, Schaffer PA, Spencer CA, Rice SA (1999) ICP22 and the UL13 protein kinase are both required for herpes simplex virus-induced modification of the large subunit of RNA polymerase II. J Virol 73:5593–5604

Marsden HS, Stow ND, Preston VG, Timbury MC, Wilkie NM (1978) Physical mapping of herpes simplex virus-induced polypeptides. J Virol 28:624–642

McGeoch DJ, Dolan A, Donald S, Rixon FJ (1985) Sequence determination and genetic content of the short unique region in the genome of herpes simplex virus type 1. J Mol Biol 181:1–13

O'Toole JM, Aubert M, Kotsakis A, Blaho JA (2003) Mutation of the protein tyrosine kinase consensus site in the herpes simplex virus 1 alpha22 gene alters ICP22 posttranslational modification. Virology 305:153–167

Ogle WO, Roizman B (1999) Functional anatomy of herpes simplex virus 1 overlapping genes encoding infected-cell protein 22 and US1.5 protein. J Virol 73:4305–4315

Poffenberger KL, Idowu AD, Fraser-Smith EB, Raichlen PE, Herman RC (1994) A herpes simplex virus type 1 ICP22 deletion mutant is altered for virulence and latency in vivo. Arch Virol 139:111–119

Pomeranz LE, Blaho JA (2000) Assembly of infectious Herpes simplex virus type 1 virions in the absence of full-length VP22. J Virol 74:10041–10054

Post LE, Roizman B (1981) A generalized technique for deletion of specific genes in large genomes: alpha gene 22 of herpes simplex virus 1 is not essential for growth. Cell 25:227–232

Prod'hon C, Machuca I, Berthomme H, Epstein A, Jacquemont B (1996) Characterization of regulatory functions of the HSV-1 immediate-early protein ICP22. Virology 226:393–402

Purves FC, Ogle WO, Roizman B (1993) Processing of the herpes simplex virus regulatory protein alpha 22 mediated by the UL13 protein kinase determines the accumulation of a subset of alpha and gamma mRNAs and proteins in infected cells. Proc Natl Acad Sci USA 90:6701–6705

Rice SA, Long MC, Lam V, Schaffer PA, Spencer CA (1995) Herpes simplex virus immediate-early protein ICP22 is required for viral modification of host RNA polymerase II and establishment of the normal viral transcription program. J Virol 69:5550–5559

Roizman B, Knipe DM (2001) Herpes simplex viruses and their replication. In: Knipe DM, Howley PM (eds) Virology. Lippincott-Raven, Philadelphia, PA, pp 2399–2459

Sears AE, Halliburton IW, Meignier B, Silver S, Roizman B (1985) Herpes simplex virus 1 mutant deleted in the alpha 22 gene: growth and gene expression in permissive and restrictive cells and establishment of latency in mice. J Virol 55:338–346

Spencer CA, Dahmus ME, Rice SA (1997) Repression of host RNA polymerase II transcription by herpes simplex virus type 1. J Virol 71:2031–2040

Tanaka M, Kagawa H, Yamanashi Y, Sata T, Kawaguchi Y (2003) Construction of an excisable bacterial artificial chromosome containing a full-length infectious clone of herpes simplex virus type 1: viruses reconstituted from the clone exhibit wild-type properties in vitro and in vivo. J Virol 77:1382–1391